Supplementary Information:

Table S1. Biogeochemical provinces and their principal characteristics used in this study from Longhurst (2010)

Region	Acronym	Cruise	North boundary	South Boundary	East Boundary	West Boundary	Ecology	Physical properties
North Atlantic Subtropical	NAST	GA01	42°N SE flowing Azores Current	25-30°N Subtropical convergence	Canary current	Gulf Stream	Seasonal mixing, low productivity spring bloom (April-June)	Northern part of the anticyclonic gyre, light westerly winds and eddy fields in north, Moderate winter mixing (MLD 100-150 m)
North Atlantic Drift	NADR	GA01	56°N Oceanic Polar Front and Subarctic Front	42°N Meeting of NAD with southeast flowing Azores Current	European shelf break	45°W	Spring stratification and high production bloom (mid-April, 39-50°N)	West wind drift, deep winter mixing (MLD < 200 m)
Atlantic Arctic	ARCT	GA01	Spitzbergen	Flemish Cap	North America	45°W	Large spring phytoplankton blooms.	Comprises the two cyclonic Subpolar Gyres of the North Atlantic Ocean. Deep winter mixing.
North Atlantic Tropical Gyral	NATR	GA06	~30°N Subtropical convergence	10-12°N Conjunction of Northern Equatorial Current and Countercurrent	Canary current	Bahama Islands	No spring bloom, low productivity and chlorophyll	Weak winter mixing, shallow MLD (15-120 m)
Western Tropical Atlantic	WTRA	GA06	~10°N Northern Equatorial Countercurrent	~ 4°S South Equatorial Current	20°W	Brazilian shelf	No spring bloom and high spatial variability in production. High chlorophyll with high nutrient concentrations	Easterly trade winds and intertropical convergence zone (ITCZ), upwelling and seasonally variable Northern Equatorial Countercurrent
Eastern Tropical Atlantic	ETRA	GA08	5-10°N	5-10°S	15°W shelfbreak front along the north-south coast from Cameroon to Congo	shelf-edge front of the east-west coast of West Africa (Guinea to Nigeria)	Enhanced chlorophyll	Southeasterly trade-winds, ITCZ above the northwest corner in winter. Seasonally varying MLD as a consequence of changes in zonal wind stress.

South Atlantic Gyral	SATL	GA08	~ 4°S South Equatorial Current	~40°S Subtropical Convergence Province (raised chlorophyll by ~0.3 mg m^{-3})	Benguela current	Brazil current	Low surface chlorophyll. Highly productive eddies near boundaries	Shallow winter mixing, anticyclonic gyre, trade winds dominate, high pressure cell (20-30 ºS). Greatest MLDs (<100 m) at ~ 20 ºS. Westerly Brazil current south of gyre (35-42 ºS)
Guinea Current Coastal	GUIN	GA08	12°N Cape Roxo	18° S Cape Frio	West African tropical coast along Congo and Angola	Shelf edge front at ca. 2-3°N 4°W	Oligotrophic area.	Shallow mixed layer above sharp and permanent thermocline. Strongly seasonal reversal of wind patterns.
Benguela Coastal Current	BENG	GA08	18°S	Cape of Good Hope	Southwestern Africa shelf	SATL	High primary productivity.	Agulhas retroflection area. Large upwelling area
Eastern Africa Coastal	EAFR	GA10	5°S Coastal boundary of Indian Ocean	Cape of Good Hope	Western boundary currents	BENG	High seasonal variability in chlorophyll concentrations	Shelf region with seasonal variability. Retroflection of the Agulhas Current.
South Subtropical Convergence	SSTC	GA10	35°S South Atlantic Gyre	45°S ACC	FKLD	EAFR	High nutrient low chlorophyll. Enhanced phytoplankton biomass in austral spring and midsummer.	Between anticyclonic circulation of the South Atlantic and cyclonic circulation of the Antarctic circumpolar Current. Strong convergence and downwelling occurring
South West Atlantic Shelf	FKLD	GA10	38°S Mar del Plata	55°S Tierra del Fuego	Argentine shelf	SSTC	High seasonal variability in chlorophyll concentrations	Two singularities: Subantarctic Front and confluence of Brazil Current and Malvinas Current.

Table S2: Sampling and analysis approaches used for each of the cruise

Cruise	Sampling CTD	Bottle	Filter type	Pore size	Air vs N_2	Reference material	Values measured reference material (nM)
GA01	Trace metal clean Rosette (TMR, General Oceanics Inc. Model 1018 Intelligent Rosette)	GO-FLO	Sartobran 300, Sartorius	0.2 µM	N_2 (0.5 bar)	GD Safe S	17.79 ± 0.26 (n=4) 1.85 ± 0.33 (n=9)
GA06	Titanium frame clean CTD Rosette	10 L Teflon coated OTE	AcroPak Supor filter capsule (Pall Corp.)	0.2 µM	Oxygen free N_2 (0.1-0.5 bar)	GD GS	18.8 ± 0.8 (n=4) 28 ± 5 (n=7)
GA08	Trace metal clean CTD Rosette	12 L GO-FLO (OTE)	Acropak 500 cartridge filters (Pall Corp.)	0.2-0.8 µM	N_2 (0.2 bar)	GS	27.8 ± 0.2 (n=4)
GA10	Titanium frame clean CTD Rosette	10 L Teflon coated OTE	AcroPak Supor polyethersulfone membrane filter capsules (Pall Corp.)	0.2 µM	High purity air (1.7 bar)	SAFe S SAFe D2	1.68 ± 0.49 (n=3) 0.89 ± 0.09 (n=4)

Table S3: Definition of the regions based on baker et al., (2013) to derive Al fractional solubility. Figure S2 shows the location of the aerosol source region and air mass type sub-regions. The last column displays the weighted average of Al fractional solubility. The different air mass types are as follow: NAr, North Atlantic remote; NAm, North America; SAf, South African; SAr, South Atlantic remote; SAbb, South African burning biomass; Sah, Saharan; SAm, South American.

Cruise	Stations	Aerosol source region	Air mass type sub-region	Air mass type %	Al fractional solubility percentage
GA01	1 to 26	2	2a	NAr 77 European 15 NAm 8	11.6
GA01	29 to 71	-	-	NAr	21
GA01	77 and 78	-	-	Canadian	14.5
GA06	7 to 9	3	3b	SAf 47 SAr 44 SAbb 7	5.8
GA06	10	4	4a	SAf 82 SAbb 17	5.5
GA06	11.5 to 18	3	3a	NAr 31 Sah 21 SAf 25	5

				SAbb 16	
GA06	19 and 20	2	2d	Sah 48 NAr 46 Eur 6	8.6
GA08	1 to 5 & 30 to 52	4	4c	SAr 81 SAf 14 SAbb 5	10.3
GA08	6 to 29	4	4b	SAf 44 SAbb 31 SAr 25	7.7
GA10	1 to 3	4	4d	SAr 94	10.9
GA10	7 to 24	5	5b	SAr 52 SAm 45	13.9

Table S4: Calculated MLD (m), measured dAl concentrations (nM), and derived atmospheric aerosol deposition estimates (g $m^{-2}yr^{-1}$) for each of the stations along the four cruises.

Cruise	Station number	MLD	dAl	Deposition flux
GA01	1	35.8	15.8	1.2
GA01	2	31.4	19.6	1.5
GA01	4	33.4	19.4	1.4
GA01	11	52.1	5.3	0.4
GA01	13	45.9	4.0	0.3
GA01	15	51.9	2.9	0.2
GA01	17	52.1	1.5	0.1
GA01	19	52.4	2.6	0.2
GA01	21	67.5	4.9	0.4
GA01	23	72.1	4.1	0.3
GA01	25	82.0	5.2	0.4
GA01	26	78.2	1.8	0.1
GA01	29	64.3	1.3	0.1
GA01	32	62.0	3.2	0.2
GA01	34	78.5	3.7	0.3
GA01	36	97.5	3.1	0.2
GA01	38	97.4	3.9	0.3
GA01	40	82.5	3.1	0.2
GA01	42	78.7	1.1	0.1
GA01	44	89.9	0.9	0.1
GA01	49	124.5	3.2	0.2
GA01	53	51.6	10.4	0.8
GA01	56	91.3	1.8	0.1
GA01	60	84.6	3.7	0.3

GA01	61	78.9	6.7	0.5
GA01	63	116.4	3.6	0.3
GA01	64	76.1	1.5	0.1
GA01	68	124.1	2.8	0.2
GA01	69	106.5	1.8	0.1
GA01	71	60.6	2.3	0.2
GA01	77	20.7	1.6	0.1
GA01	78	12.0	0.9	0.1
GA06	7	35.6	15.6	2.2
GA06	8	46.4	8.1	1.1
GA06	9	42.4	24.0	3.4
GA06	10	51.3	8.8	1.2
GA06	11.5	43.4	15.0	2.1
GA06	12	32.6	17.3	2.5
GA06	13	29.4	21.0	3.0
GA06	14	32.9	67.5	9.6
GA06	15	39.9	35.6	5.1
GA06	16	42.1	22.4	3.2
GA06	17	44.1	19.7	2.8
GA06	18	40.5	31.5	4.5
GA06	19	50.4	24.8	3.5
GA06	20	38.0	16.6	2.4
GA08	1	-	-	-
GA08	2	-	-	-
GA08	3	33.0	4.4	0.8
GA08	4	59.0	4.0	0.7
GA08	5	29.0	4.9	0.9
GA08	6	13.0	12.0	2.2
GA08	7	25.2	22.0	4.1
GA08	8	12.2	31.0	5.7
GA08	9	13.5	43.0	7.9
GA08	10	14.1	62.0	11.4
GA08	11	11.8	14.5	2.7
GA08	12	11.0	28.0	5.2
GA08	13	8.5	72.0	13.3
GA08	14	12.0	37.0	6.8
GA08	15	13.0	784.6	163.2
GA08	16	5.0	269.0	56.0
GA08	17	8.7	261.0	54.3
GA08	18	9.2	211.0	43.9
GA08	19	8.2	209.0	43.5
GA08	20	9.0	186.0	38.7
GA08	21	15.8	44.9	8.3

GA08	22	20.2	48.6	9.0
GA08	23	23.8	32	6.7
GA08	24	28.4	20.8	3.8
GA08	25	37.2	13.6	2.5
GA08	26	24.8	7.0	1.3
GA08	27	28.0	9.8	1.8
GA08	28	40.4	12.8	2.4
GA08	29	30.0	7.3	1.3
GA08	30	56.4	11.8	2.2
GA08	31	41.7	4.5	0.8
GA08	32	44.6	1.8	0.3
GA08	33	35.4	2.3	0.4
GA08	34	39.2	5.3	1.0
GA08	35	40.5	4.3	0.8
GA08	36	32.3	1.9	0.3
GA08	37	35.5	2.2	0.4
GA08	38	38.6	1.5	0.3
GA08	39	43.6	1.9	0.4
GA08	40	-	-	-
GA08	41	42.0	2.5	0.5
GA08	42	31.8	5.4	1.0
GA08	43	34.0	3.3	0.6
GA08	44	6.0	1.2	0.2
GA08	45	36.1	4.3	0.8
GA08	46	65.0	2.9	0.5
GA08	47	12.0	8.3	1.5
GA08	48	11.0	2.2	0.4
GA08	49	12.0	4.9	0.9
GA08	50	12.0	4.7	0.8
GA08	51	19.0	4.5	0.7
GA10	1	29.3	4.4	0.3
GA10	2	32.4	4.2	0.4
GA10	3	54.4	0.7	0.0
GA10	7	65.4	0.4	0.0
GA10	8	54.1	0.7	0.1
GA10	11	62.8	0.3	0.0
GA10	12	65.1	1.9	0.1
GA10	13	65.4	0.5	0.0
GA10	14	48.1	0.7	0.1
GA10	15	56.2	0.7	0.1
GA10	16	69.9	1.6	0.1
GA10	17	71.8	2.7	0.2
GA10	18	57.9	2.0	0.1

GA10	19	51.6	1.1	0.1
GA10	20	30.5	5.2	0.3
GA10	21	46.0	12.0	0.8
GA10	22	34.0	15.8	1.0
GA10	24	28.1	5.4	0.3

Table S5: Input values to estimate total atmospheric aerosol deposition fluxes using the MADCOW model. MLD, average between the median MLDms and MLDar; τ, Al residence time derived from Han et al. (2008) for the different biogeochemical provinces; Alsol%, Al fractional solubility percentage calculated from Baker et al. (2013). For reference to the biogeochemical provinces please refer to Table S1.

Cruise	MLD (m)	τ (yr)	Alsol% range (%)
GA01	57	1.25 (NAST and NADR) 0.75 (ARCT)	11.6-20
GA06	36	1.25 (NATR and WTRA)	5-8.6
GA08	20	0.75 (BENG, GUIN, and ETRA) 3 (SATL)	7.7-10.3
GA10	47	1.5 (EAFR) 1 (SSTC and FKLD)	10.9-13.9

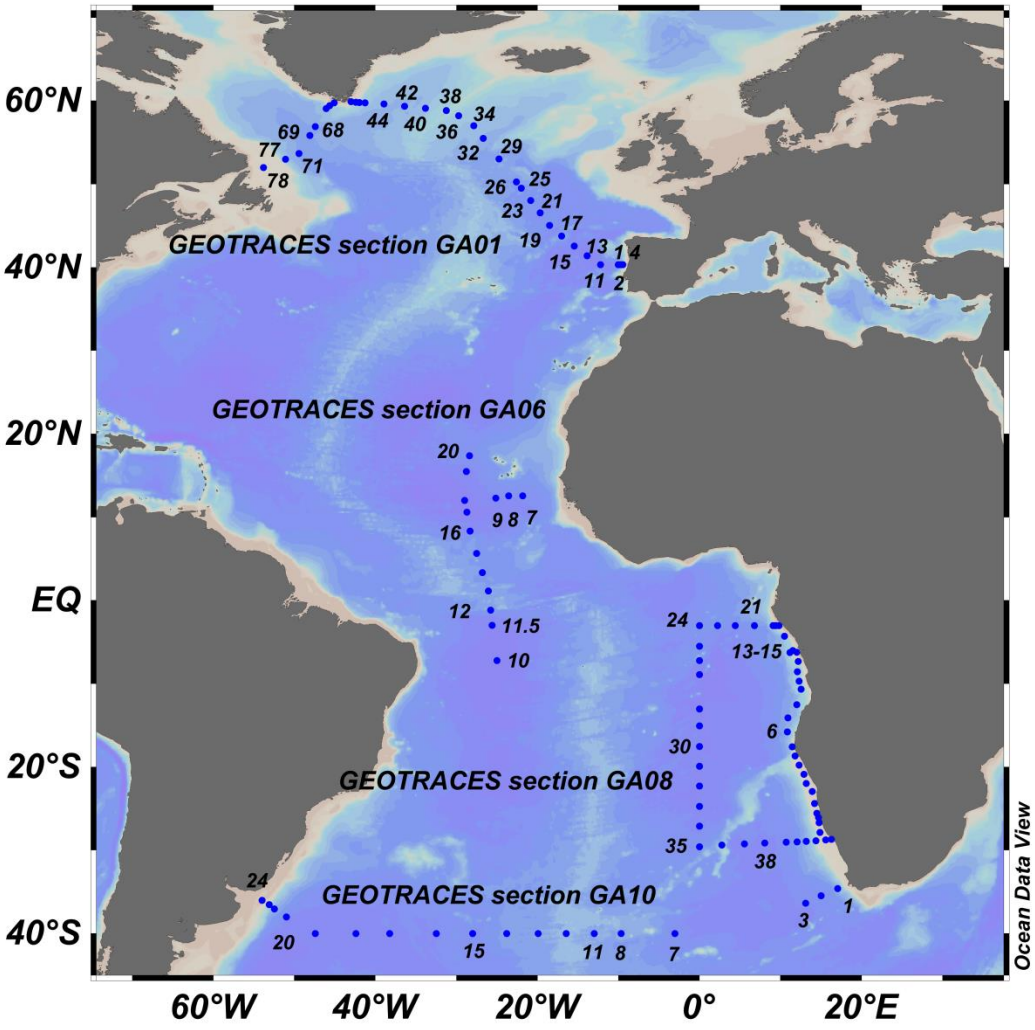

Figure S1 Map showing the cruise locations and the station numbers

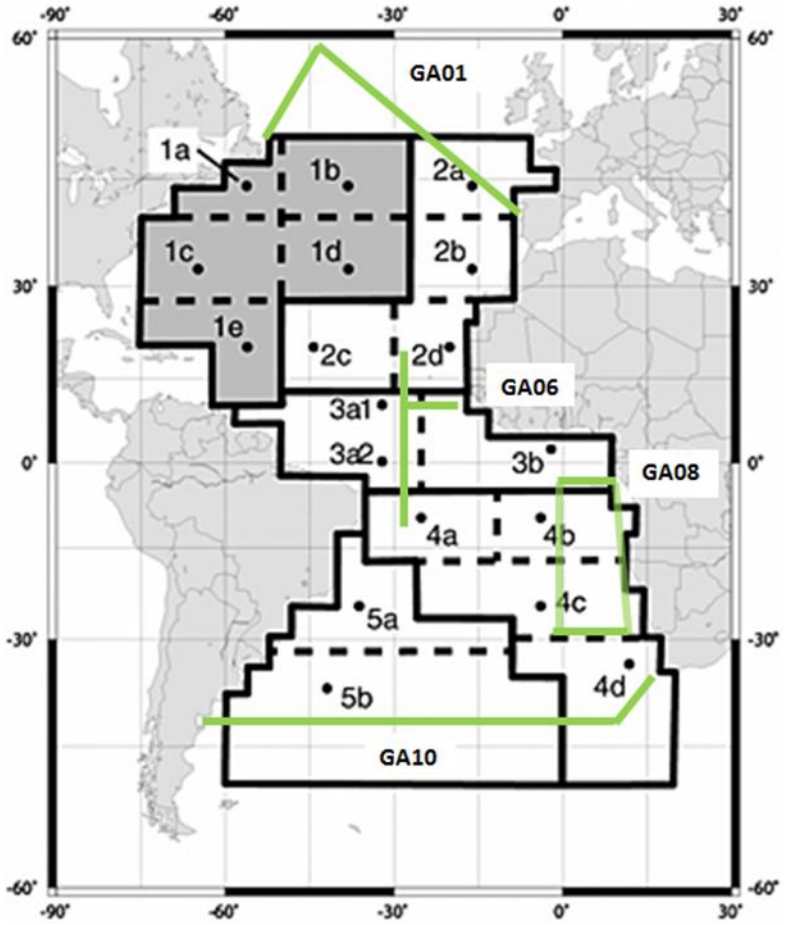

Figure S2: Atmospheric sub-regions used to define aerosol Al fractional solubility. The cruise tracks for GA01, GA06, GA08 and GA10 are plotted as green solid lines. Modified from (Baker et al., 2013).

Explanatory notes for Figure S2:

Fractional Al solubility in the North Atlantic (GA01)

In the North Atlantic, section GA01, we used a combination of in Al fractional solubility ($Al_{sol\%}$) estimates from aerosols collected during the cruise (Shelley et al., 2017) for stations north of 50°N and $Al_{sol\%}$ estimates from the compilation of Baker et al. (2013) for stations south of 50°N. For stations 1 to 26 we used an $Al_{sol\%}$ of 11.6 % as the stations fall into aerosol source region 2 and air mass type sub-region 2a. Sub region 2a is dominated by North Atlantic remote (76.8 %) and European (15.2 %) air mass types with a small and residual contribution of North American (7.8 %) and Saharan (0.25 %) air mass types, respectively. From station 29 to 71 we averaged all the aerosol $Al_{sol\%}$ estimates as all the air mass types for the aerosol samples collected (n=9) between the previous mentioned stations had a North Atlantic remote air mass provenance yielding a final $Al_{sol\%}$ of 21 %. The last two stations (77 and 78) were located between aerosol samples geoa17 and geoa18 which had a Canadian air mass type origin with an average $Al_{sol\%}$ of 14.5 %.

Fractional Al solubility in the tropical Atlantic (GA06)

For the tropical Atlantic, section GA06, we selected four different $Al_{sol\%}$ values. For the eastward transect (stations 7 to 9) an $Al_{sol\%}$ of 5.8 % was selected as the stations were located in the aerosol source region number 3. Air mass provenance within sub-region 3b were Southern African (46.5%) and South Atlantic remote (43.6%), with a small contribution of Southern African biomass burning (7.1%) and Sahara (2.7%)

air mass types and a residual contribution of North Atlantic remote (0.2%) air mass type. The most southern station (station 10) was located within source region 4 and air mass provenance within sub-region 4a. Sub-region 4a was dominated by Southern African (82.1%) and Southern African biomass burning (16.9%) air mass types with an additional small contribution of Southern Atlantic remote (1.1%) air mass type, thus yielding an $Al_{sol\%}$ of 5.5 %. Similar to station 10, for the northward transect (St. 11.5 to 18) we used an $Al_{sol\%}$ of 5 %. This northward transect was located in aerosol source region 3, although the air mass type provenance was a combination between sub regions 3a1 and 3a2. Sub-region 3a (3a1+3a2) had a mixed air mass type provenance, with North Atlantic remote (30.5 %), Sahara (20.7 %), Southern African (24.9 %) and Southern Atlantic biomass burning (15.5 %) dominating the air mass types. A small contribution of Southern Atlantic remote (9.1 %) and European (0.2 %) was also present. The most northern stations (St. 19 and 20) had the highest $Al_{sol\%}$ with a value of 8.6 % as they were located in aerosol source region 2 and air mass type provenance sub-region 2d, which is dominated by Sahara (48.1. %) and North Atlantic remote (45.7 %) air mass types. Sub-region 2d also had a small and residual contribution of European (6 %) and North American (0.3 %) air mass types, respectively.

Fractional Al solubility in the South East Atlantic (GA08)

In the South East Atlantic, section GA08, two different $Al_{sol\%}$ were used. Both were located in aerosol source region 4. Stations 1 to 5 and 30 to 52 were located in air mass type sub-region 4c. Sub-region 4c was dominated by Southern Atlantic remote (81.2 %) and South African (13.5 %) air mass types with smaller contributions of Southern Africa burning biomass (4.9 %) and South American (0.5 %) air mass types, yielding an average $Al_{sol\%}$ of 10.3 %. Stations 6 to 29 were located in air mass type sub-region 4b, where the dominant air type masses were Southern Africa (44.2 %), Southern Africa burning biomass (30.8 %) and Southern Atlantic remote (25.1 %). Average $Al_{sol\%}$ for sub-region 4b was 7.7 %.

Fractional Al solubility in the South Atlantic Ocean (GA10)

For the Southern Ocean (GA10), two different $Al_{sol\%}$ were used. On the eastern part of the transect, stations 1 to 3, we used a value of 10.9 % which is mainly due to 94.3 % of the air masses types having a South Atlantic remote areas origin with an average $Al_{sol\%}$ of 11.3. West of station 3, stations 7 to 24, we used an $Al_{sol\%}$ of 13.9 % which is mainly due to the combined effect of 52 % and 45 % of the air masses coming from South Atlantic marine remote areas and South America with an average $Al_{sol\%}$ of 14.1 % and 14.5 %, respectively.

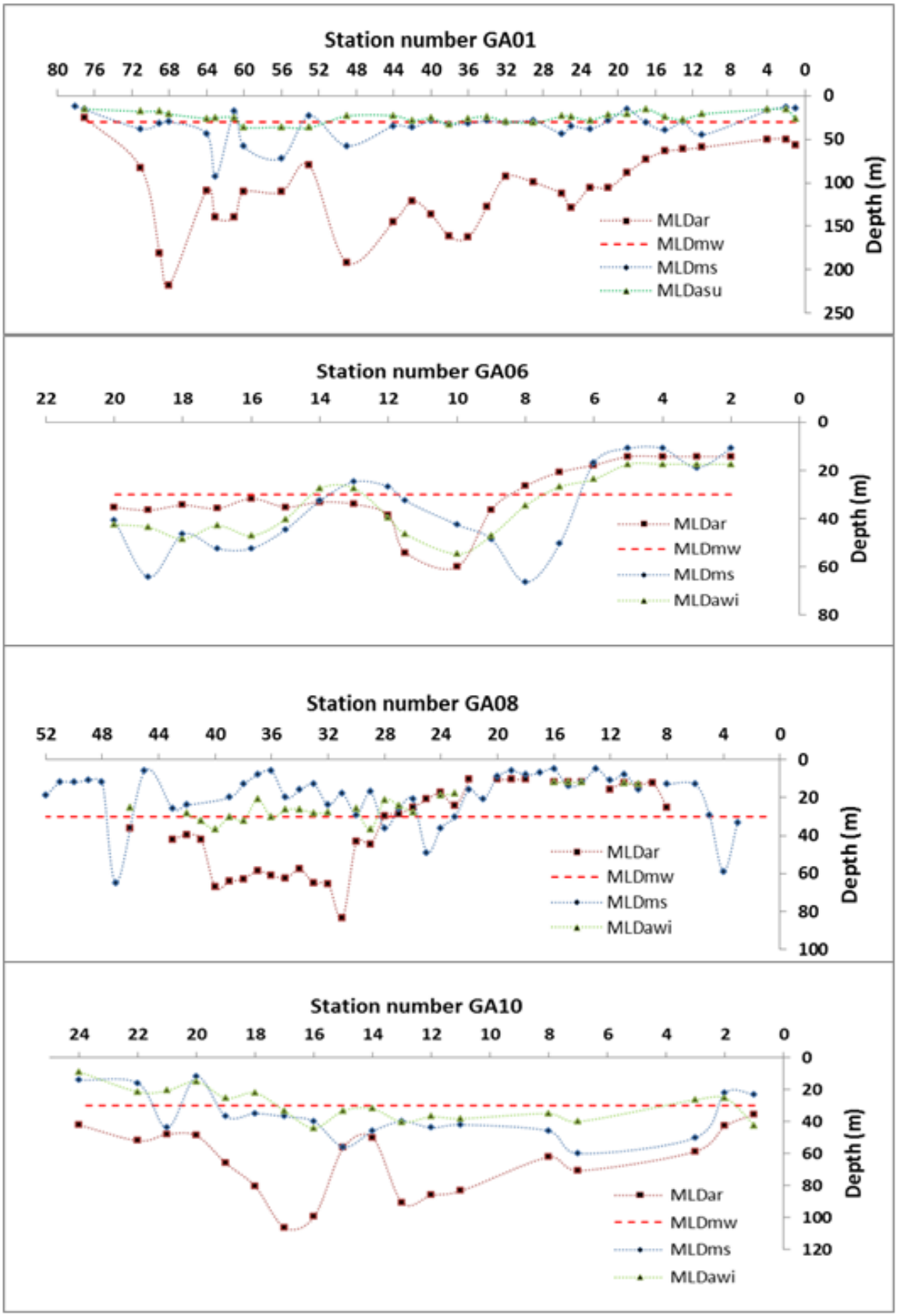

Figure S3 Depth of the surface mixed layer (MLD). MLDar refers to the annual average MLD from the Argo project (Holte et al., 2017). MLDms refers to in situ MLD measured on each cruise. MLDasu or MLDawi represent the summer or winter average MLD from the Argo project. MLDmw represent the MLD used in the original application of the MADCOW model (30 m) (Measures et al., 2015).

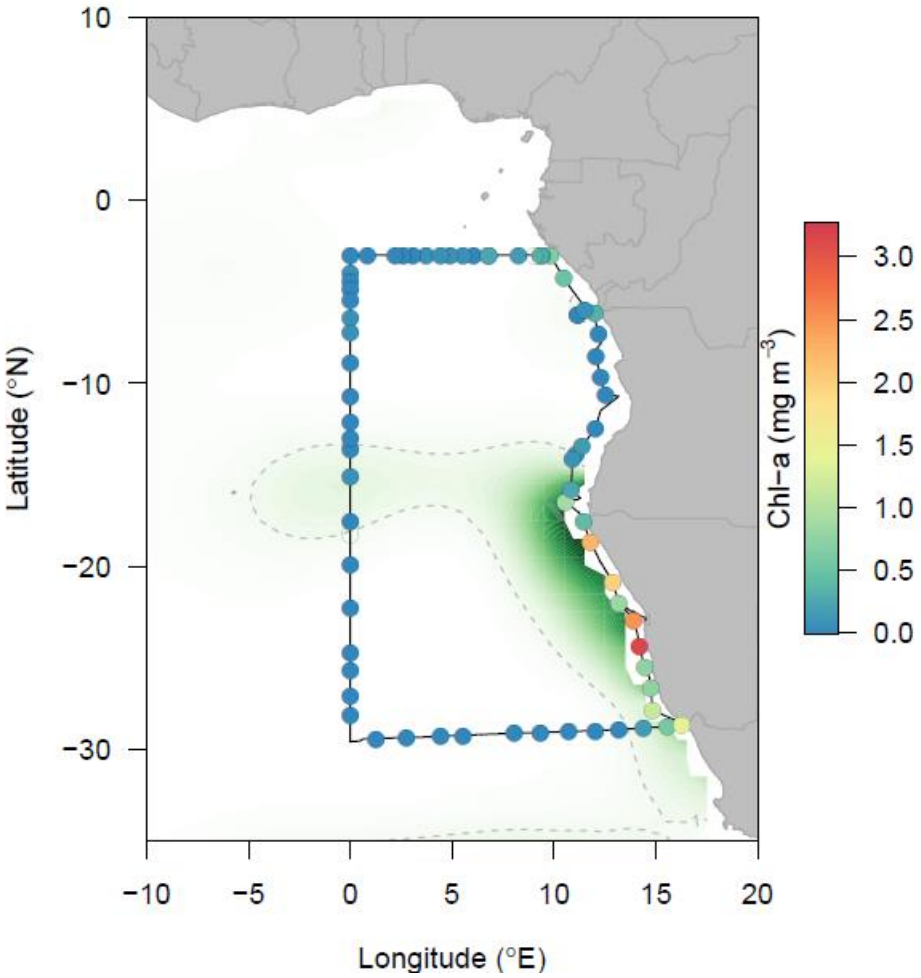

Figure S4 Chlorophyll a values for GEOTRACES section GA08. Data are from Dr. Tom Browning.

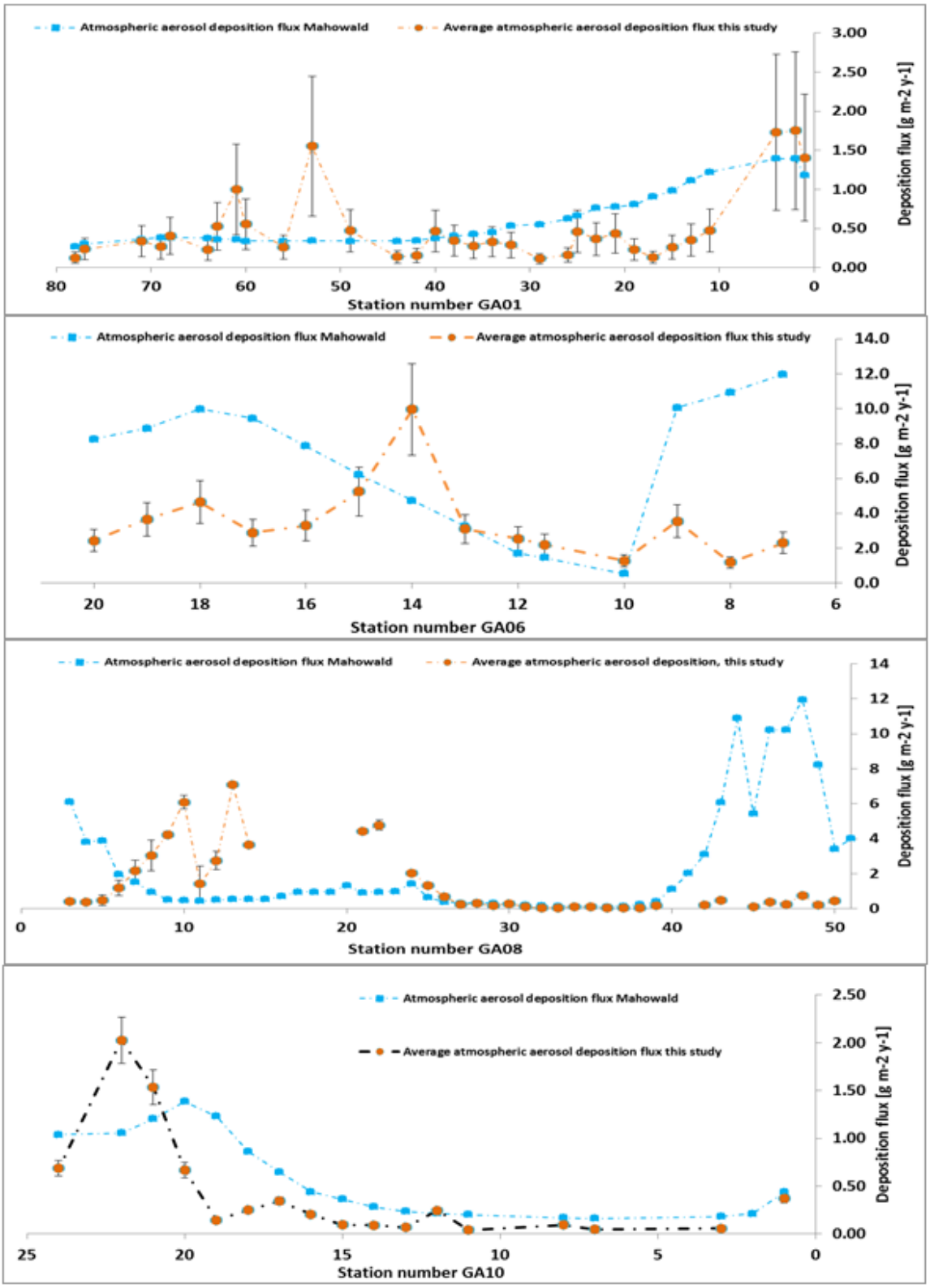

Figure S5: Total average atmospheric aerosol deposition fluxes (this study) and model atmospheric aerosol deposition estimates from Mahowald et al. (2005).

Baker, A., Adams, C., Bell, T., Jickells, T., and Ganzeveld, L.: Estimation of atmospheric nutrient inputs to the Atlantic Ocean from 50° N to 50° S based on large-scale field sampling: Iron and other dust-associated elements, Global Biogeochemical Cycles, 27, 755-767, 2013.
Holte, J., Talley, L. D., Gilson, J., and Roemmich, D.: An Argo mixed layer climatology and database, Geophysical Research Letters, 2017. 2017.
Longhurst, A. R.: Ecological geography of the sea, Academic Press, 2010.

Mahowald, N. M., Baker, A. R., Bergametti, G., Brooks, N., Duce, R. A., Jickells, T. D., Kubilay, N., Prospero, J. M., and Tegen, I.: Atmospheric global dust cycle and iron inputs to the ocean, Global Biogeochemical Cycles, 19, 2005.
Measures, C., Hatta, M., Fitzsimmons, J., and Morton, P.: Dissolved Al in the zonal N Atlantic section of the US GEOTRACES 2010/2011 cruises and the importance of hydrothermal inputs, Deep Sea Research Part II: Topical Studies in Oceanography, 116, 176-186, 2015.
Shelley, R. U., Landing, W. M., Ussher, S. J., Planquette, H., and Sarthou, G.: Characterisation of aerosol provenance from the fractional solubility of Fe (Al, Ti, Mn, Co, Ni, Cu, Zn, Cd and Pb) in North Atlantic aerosols (GEOTRACES cruises GA01 and GA03) using a two stage leach, Biogeosciences Discuss., 2017, 1-31, 2017.